

# Technical note: The MESSy-submodel AIRSEA calculating the air-sea exchange of chemical species

A. Pozzer, P. Jöckel, R. Sander, L. Ganzeveld, and J. Lelieveld

Max Planck Institute for Chemistry, Mainz, Germany

Received: 15 June 2006 – Accepted: 19 July 2006 – Published: 29 August 2006

Correspondence to: A. Pozzer (pozzer@mpch-mainz.mpg.de)

Title Page

Abstract

Introduction

Conclusions

References

Tables

Figures

◀

▶

◀

▶

Back

Close

Full Screen / Esc

Printer-friendly Version

Interactive Discussion

EGU

## Abstract

The new submodel AIRSEA for the Modular Earth Submodel System (MESSy) is presented. It calculates the exchange of chemical species between the ocean and the atmosphere with a focus on organic compounds. The submodel can be easily extended to a large number of tracers, including highly soluble ones. It is demonstrated that application of explicitly calculated air-sea exchanges with AIRSEA can induce substantial changes in the simulated tracer distributions in the troposphere in comparison to a model version in which this process is neglected. For example, the simulations of acetone, constrained with measured oceanic concentrations, shows relative changes in the atmospheric surface layer mixing ratios over the Atlantic Ocean up to 300%.

## 1 Introduction

Recently, increasing attention has been given to gas exchange between the ocean and the atmosphere. Oceans have generally been considered very important for the atmosphere (e.g. for moisture and heat transport), while in the last decade their significance for the budgets of many atmospheric chemical species (tracers) has also been recognised, with an increasing interest in volatile organic compounds (VOC) and their oxidation products (OVOC) (Singh et al., 2001; Marandino et al., 2005; Plass-Dülmer et al., 1995). So far, modelling studies of global air-sea exchanges, focusing on organic compounds, have only been performed for a few specific cases and/or tracers (e.g. Carpenter et al., 2004, Berner et al., 2003 or Kettle and Andreae, 2000), whereas no comprehensive simulations with general circulation models (GCMs) have been performed. The atmosphere-ocean exchange of gases is critical for a good representation of many OVOCs in the troposphere and hence of ozone and other oxidants.

Here we present AIRSEA, a new submodel for the Modular Earth Submodel System (MESSy) (Jöckel et al., 2005). AIRSEA is used to calculate these exchange processes in global models. The submodel has been tested mainly with organic compounds

ACPD

6, 8189–8214, 2006

## MESSy AIRSEA

A. Pozzer et al.

Title Page

Abstract

Introduction

Conclusions

References

Tables

Figures

◀

▶

◀

▶

Back

Close

Full Screen / Esc

Printer-friendly Version

Interactive Discussion

EGU

(methanol, acetone, propane, propene) and a few others, e.g., CO<sub>2</sub>, DMS, SO<sub>2</sub>.

However, due to its generality, AIRSEA can be easily extended to many tracers with only a few restrictions, for example, acids and bases with a pH-dependent solubility, for which aqueous phase dissociation needs to be considered.

## 2 Submodel description

In AIRSEA, the two-layer model presented by [Liss and Slater \(1974\)](#) has been adopted. This model is based on the assumption that close to the air-sea interface each fluid is well mixed, and that within the interface between water and air the exchange is solely driven by molecular diffusion. The two layer model has been used to introduce a first more mechanistic representation of air-sea exchanges where more recent approaches will be used in the future (e.g. [Asher and Pankow, 1991](#)).

The model input includes concentrations in the uppermost ocean layer, where the fluid is well mixed by turbulence (due to wind stress). Assuming further that transport of gases across the interface is a steady state process, it follows ([Liss and Slater, 1974](#)) that the flux  $F$  (in mol/(m<sup>2</sup>s)) across the interface is

$$F = K_{\text{tot}}(c_w - Hp_g) \quad (1)$$

where  $c_w$  is the concentration of the tracer in water (in mol/m<sup>3</sup>),  $H$  is the Henry's Law coefficient (in mol/(m<sup>3</sup>Pa)),  $p_g$  is the partial pressure (in Pa) of the gas in air over the liquid surface and  $K_{\text{tot}}$  is the transfer (or piston) velocity (in m/s).

The Henry's Law coefficient  $H$  is calculated (including the temperature dependence ([Sander, 1999a–1999b](#), and reference therein). We define the Henry's Law coefficient as the ratio of the aqueous-phase concentration of a species to the partial pressure of the same species in the gas phase. Hence some of the following equations read slightly different in comparison to those in the original references, mostly due to the different definition of the Henry's Law coefficient.

Title Page

Abstract

Introduction

Conclusions

References

Tables

Figures

◀

▶

◀

▶

Back

Close

Full Screen / Esc

Printer-friendly Version

Interactive Discussion

$K_{\text{tot}}$  can be defined as (Liss and Slater, 1974):

$$K_{\text{tot}} = (R_g + R_w)^{-1} = \left( \frac{1}{\alpha K_w} + \frac{HRT}{K_g} \right)^{-1}, \quad (2)$$

$$\frac{HRT}{K_g} = R_g, \quad (3)$$

$$\frac{1}{\alpha K_w} = R_w. \quad (4)$$

$\alpha$  is an enhancement factor due to the species reaction in solution (dimensionless),  $R$  is the gas constant (in  $\text{J mol}^{-1} \text{K}^{-1}$ ),  $T$  is the temperature (in K),  $K_w$  and  $K_g$  are exchange constants for the liquid and gas phase (in m/s),  $R_g$  and  $R_w$  (in s/m) are the resistances in the gas and liquid phase, respectively.

The salinity effect on the tracer's solubility is taken into account using the Setschenow equation :

$$\ln \left( \frac{H}{H_0} \right) = -K_s c_s, \quad (5)$$

where  $K_s$  is the Setschenow (or salting out) constant (in  $\text{m}^3/\text{mol}$ ),  $c_s$  (in  $\text{mol}/\text{m}^3$ ) is the concentration of the salt in ocean water, and  $H_0$  is the Henry's Law coefficient in distilled water. Xie et al. (1997) showed that for organic tracers the Setschenow constant  $K_s$  can be approximated as

$$K_s = 0.0018 V_x, \quad (6)$$

where  $V_x$  is the molar volume at the boiling point of the tracer (in  $\text{m}^3/\text{mol}$ ). Xie et al. (1997) showed further that this approximation leads to better estimates of  $K_s$ , compared to various experimental methods, which require assumptions about several parameters (Xie et al., 1990). However, it is highly recommended to check the calculated values with experimental data.

[Title Page](#)
[Abstract](#)
[Introduction](#)
[Conclusions](#)
[References](#)
[Tables](#)
[Figures](#)
[◀](#)
[▶](#)
[◀](#)
[▶](#)
[Back](#)
[Close](#)
[Full Screen / Esc](#)
[Printer-friendly Version](#)
[Interactive Discussion](#)

Title Page

Abstract

Introduction

Conclusions

References

Tables

Figures

◀

▶

◀

▶

Back

Close

Full Screen / Esc

Printer-friendly Version

Interactive Discussion

In AIRSEA the calculation following Eq. (6) is optionally included for all tracers, although this is strictly valid only for organics (Xie et al., 1997). Climatological global monthly average maps of salinity are taken from the World Ocean Atlas (2001), by Boyer et al. (2002), in a  $1^\circ \times 1^\circ$  resolution.

For  $K_w$  different estimates exist, primarily based on combinations of field and laboratory studies (Liss and Merlivat, 1986; Wanninkhof, 1992; Nightingale et al., 2000). In AIRSEA,  $K_w$  (in m/s) is calculated using the semi-empirical formulation proposed by Wanninkhof (1992), with a quadratic dependence on the 10-m wind speed ( $U_{10}$  in m/s):

$$K_w = \beta \times (U_{10})^2 \times \left( \frac{Sc_{liq}}{660} \right)^{-n} \quad (7)$$

with  $\beta = 2.8 \times 10^{-6} \times 0.31 \text{ s/m}$ .  $Sc_{liq}$  is the dimensionless Schmidt number (in the liquid phase). The Schmidt number is defined as  $\nu/D$ , with the kinematic viscosity  $\nu$  (in  $\text{m}^2 \text{s}^{-1}$ ) and the molecular diffusivity  $D$  (in  $\text{m}^2 \text{s}^{-1}$ ). The exponent ranges from  $2/3$  for a smooth surface to  $1/2$  for a rough or wavy surface (Jähne et al., 1987). In AIRSEA a constant value of  $n=1/2$  is used. However, due to the turbulent characteristics of the top ocean layer and the presence of bubbles which can enhance the transfer, we adopted in addition to Eq. (7), an alternative parametrisation with an empirical coefficient for non-clean bubbles in the presence of white-caps (Asher and Wanninkhof, 1998a):

$$K_w = \left[ (\kappa U_{10} + W_c (115200 - \kappa U_{10})) Sc_{liq}^{-1/2} + W_c \left( \frac{-37}{\alpha_{ost}} + 6120 \alpha_{ost}^{-0.37} Sc_{liq}^{-0.18} \right) \right] \times 2.8 \times 10^{-6} \text{ m/s} \quad (8)$$

where  $\alpha_{ost}$  is the dimensionless Ostwald number and  $\kappa = 47 \text{ s/m}$ . The fractional area coverage  $W_c$  of actively breaking white-caps is defined as (Monahan, 1993; Soloviev

and Schluessel, 2002):

$$W_c = c_1(U_{10} - c_0)^3 \quad (9)$$

with  $c_1=2.56 \times 10^{-6} \text{ s}^3 \text{ m}^{-3}$  and  $c_0=1.77 \text{ ms}^{-1}$ .

The two alternatives (Eqs. 7 and 8) are selectable via the user interface (Fortran90 namelist); changes of the submodel code are not required.

It has to be stressed that Eq. (8) is strictly valid only for gases far from equilibrium (Asher and Wanninkhof, 1998a, Asher and Wanninkhof, 1998b).

The effect of bubbles on the transfer velocity has been characterised by Asher and Wanninkhof (1998a), which changes the exponent in Eq. (7), as pointed out by Asher and Wanninkhof (1998b). This influence on the exponent is very important for soluble gases. However, the understanding of this phenomenon is poor for gases close to equilibrium, and no parameterisation for the bubble entrainment is generally accepted. Hence a constant exponent of  $n=1/2$  is used in Eq. (7).

Since precipitation can significantly increase the air-sea exchange, a parameterisation has been adopted (Ho et al., 2004), and the resulting transfer velocity has been added to the calculated  $K_w$  only in the presence of rain ( $K_w=K_w+K_w^{(p)}$ ):

$$K_w^{(p)} = k_d \times (k_a + k_b R_n - k_c R_n^2) \times \left( \frac{S C_{\text{liq}}}{600} \right)^{-n} \quad (10)$$

where the superscript ( $p$ ) denotes “precipitation”,  $R_n$  is the rain rate in mm/h and  $K_w^{(p)}$  is in m/s. Here  $k_a=0.929$ ,  $k_b=0.679 \text{ h/mm}$ ,  $k_c=0.0015 \text{ h}^2/\text{mm}^2$ , and  $k_d=2.8 \times 10^{-6} \text{ m/s}$ . The rain rate is obtained from other submodels for convective and large scale clouds. As pointed out by Ho et al. (2004) more studies are required in this field, and the implementation of this feature has been included (selectable via the user interface). By default, it is not activated.

For very soluble gases the gas phase can play a key role as a resistance against the

Title Page

Abstract

Introduction

Conclusions

References

Tables

Figures

◀

▶

◀

▶

Back

Close

Full Screen / Esc

Printer-friendly Version

Interactive Discussion

exchange (see Eq. 3). The value of  $K_g$  is given by [Carpenter et al. \(2004\)](#):

$$K_g = \frac{1}{R_1 + R_2}, \quad (11)$$

where  $R_1$  is the aerodynamic resistance and  $R_2$  is the gas-phase film resistance (both in s/m). Assuming a neutrally stable atmospheric surface layer, [Garland \(1977\)](#) used

$$R_1 = \frac{U(z)}{u_*^2}, \quad (12)$$

where  $U(z)$  is the wind speed at the height  $z$  of the lowest model layer and  $u_*$  is the friction velocity (both in m/s). Further, the gas phase resistance is given by [Wesely \(1989\)](#) as

$$R_2 = \left(\frac{5}{u_*}\right) Sc_{\text{air}}^{2/3}, \quad (13)$$

where  $Sc_{\text{air}}$  is the dimensionless Schmidt number in air.

The Schmidt number in water is estimated from the Schmidt number for  $\text{CO}_2$ . This approach is preferred to other methods, e.g., from direct measurements ([Saltzman et al., 1993](#)), because these are not always available, and also because the parameterisation of  $K_w$  has been mainly derived from  $\text{CO}_2$  measurements. Therefore, the Schmidt number for species  $x$  is

$$Sc_x = \left(\frac{\nu}{D_x}\right) = Sc_{\text{CO}_2} \left(\frac{D_{\text{CO}_2}}{D_x}\right). \quad (14)$$

An expression for  $D_{\text{CO}_2}/D_x$  can be obtained ([Hayduk and Laudie, 1974](#) or [Wilke and Chang, 1955](#)):

$$\frac{D_{\text{CO}_2}}{D_x} = \left(\frac{V_x}{V_{\text{CO}_2}}\right)^{0.6} \quad (15)$$

Title Page

Abstract

Introduction

Conclusions

References

Tables

Figures

◀

▶

◀

▶

Back

Close

Full Screen / Esc

Printer-friendly Version

Interactive Discussion

where  $V_x$  and  $V_{\text{CO}_2}$  are the molar volumes of the tracer and of  $\text{CO}_2$  at their boiling points at standard pressure, respectively. With this, a more realistic temperature dependence of the Schmidt number on the temperature of the sea-water is achieved. Finally, the Schmidt number for  $\text{CO}_2$  can be calculated using the relation given by Wanninkhof

(1992) obtained for sea-water

$$Sc_{\text{CO}_2} = k_0 - k_1 T + k_2 T^2 - k_3 T^3 \quad (16)$$

with  $T$  (temperature) in K and  $k_0=2073.1$ ,  $k_1=125.62$  (1/K),  $k_2=3.6276$  (1/K<sup>2</sup>), and  $k_3=0.043219$  (1/K<sup>3</sup>).

The diffusivity (in m<sup>2</sup>s<sup>-1</sup>) of a tracer in air is calculated following the Fuller, Schettler and Giddings (FSG) method (Lyman et al., 1990):

$$D_x = k \frac{10^{-11} T^{1.75} \sqrt{\frac{M_{\text{air}} + M_x}{M_{\text{air}} M_x}}}{\rho \left[ V_{\text{air}}^{o1/3} + V_x^{o1/3} \right]^2} \quad (17)$$

where  $V_x^o$  is the molar volume based on the method developed by Fuller (in m<sup>3</sup>/mol) which is equal to 0.8745 times the molar volume at boiling point, and  $V_{\text{air}}^o$  is  $20.1 \times 10^{-6}$  (m<sup>3</sup>/mol).  $T$  is the air temperature (in K),  $M_{\text{air}}$  and  $M_x$  are the molar masses of air and the tracer, respectively.  $k=101\,325 \text{ Pa m}^4 \text{ g}^{0.5} \text{ s}^{-1} \text{ mol}^{-1.167} \text{ K}^{-1.75}$  is a constant used to obtain the right unit system.

## 2.1 Time scale

Ultimately, the change of concentration  $c_x$  of a tracer  $x$  in air above the ocean, is described by

$$\frac{dc_x(t)}{dt} = \frac{K_{\text{tot}}}{z} (c_w - c_x) \quad (18)$$

[Title Page](#)
[Abstract](#)
[Introduction](#)
[Conclusions](#)
[References](#)
[Tables](#)
[Figures](#)
[◀](#)
[▶](#)
[◀](#)
[▶](#)
[Back](#)
[Close](#)
[Full Screen / Esc](#)
[Printer-friendly Version](#)
[Interactive Discussion](#)

where  $c_w$  is the concentration of the tracer in the ocean water and  $z$  is the height of the lowest model layer. This equation can be solved analytically, yielding

$$c_x(t) = c_0 e^{-\gamma t} + (1 - e^{-\gamma t}) c_w \quad (19)$$

with  $\gamma = \frac{K_{\text{tot}}}{z}$ . Eq. (19) shows the typical time scale of the exchange process:  $\tau = 1/\gamma$ .

This time scale depends on the tracer and the vertical model resolution.

As an example, Fig. 1 depicts the time scale  $\tau$  for  $\text{CO}_2$ . The magnitude of  $\tau$  for this tracer is on the order of days to weeks; however, a large spatial variability is apparent. The shortest time scale (and hence highest transfer velocity) occurs in the storm track region, where high wind speeds are common. It has to be stressed that this is strictly valid only for this specific tracer. In case of a very soluble gas, in contrast, the temperature dependence of  $K_{\text{tot}}$  can lead to a different result. The highest emission/deposition velocities are located in the tropical regions (where the ocean is warmest) and not where the highest wind speed occurs. Figure 2 depicts the transfer velocity for a soluble tracer (methanol), which shows the strong dependence of the transfer velocity on the temperature of the sea surface.

### 3 Implementation as MESSy submodel

The implementation of the submodel AIRSEA described in Sect. 2 strictly follows the MESSy (Modular Earth Submodel System) standard (Jöckel et al., 2005); hence application to a general circulation model (GCM) is straightforward. AIRSEA is part of the MESSy model and available to the community. For details how to obtain the code, see <http://www.messy-interface.org>. The AIRSEA submodel, together with DRYDEP, OFFLEM, ONLEM, EMDEP and TNUDGE, accounts for the emission-deposition processes in the model. AIRSEA provides either a source or a sink of a tracer, following Eq. (1), depending on its concentrations in water and air. Particular attention has to be paid to other emission submodels to avoid double counting. Variables required for

Title Page

Abstract

Introduction

Conclusions

References

Tables

Figures

◀

▶

◀

▶

Back

Close

Full Screen / Esc

Printer-friendly Version

Interactive Discussion

the calculation of the transfer velocity  $K_{\text{tot}}$  (wind speed at 10 m ( $U_{10}$ ), pressure, temperature (of air and surface), friction velocity ( $u_*$ )) are imported from the GCM via the MESSy data interface. The parameters specific for each tracer (e.g. molar volume at boiling point, Henry's Law coefficient, and molar mass) are provided via the user interface (Fortran90 namelist). This flexibility allows a large number of different studies without requiring a recompilation of the code. For instance, the calculation can also be performed for idealised tracers in process studies. The concentration of a specific tracer in ocean water, which is required for the calculation, can be

- provided by the user as constant value,
- provided from prescribed maps (e.g., climatologies) imported via the MESSy sub-model OFFLEM (Kerkweg et al., 2006), or
- provided directly (“online”) by ocean chemistry submodels.

In a model simulation including AIRSEA, the tracer concentrations (in air) are changed according to the air-sea exchange process (Eq. 18). In every grid box of the lowest model layer, an additional tracer tendency is calculated

$$\frac{\Delta c_x}{\Delta t} = \frac{c_x(t + \Delta t) - c_x(t)}{\Delta t}, \quad (20)$$

where  $\Delta t$  is the model time step. The signal is then transported to higher model layers by other processes, such as advection, convection, etc.

## 4 Evaluation

As shown in Sect. 3, AIRSEA can be easily applied to many types of tracers. Nevertheless, information about the sea water concentration of the tracers is required. This can be taken from available climatologies, parameterised, or derived directly from field studies. So far, we included constant climatological concentrations for  $\text{CH}_3\text{COCH}_3$ ,

Title Page

Abstract

Introduction

Conclusions

References

Tables

Figures

◀

▶

◀

▶

Back

Close

Full Screen / Esc

Printer-friendly Version

Interactive Discussion

CH<sub>3</sub>OH, C<sub>2</sub>H<sub>6</sub>, C<sub>2</sub>H<sub>4</sub>, C<sub>3</sub>H<sub>8</sub> and C<sub>3</sub>H<sub>6</sub> from Plass-Dülmer et al. (1995), Zhou and Mopper (1997), Zhou and Mopper (1993), and Williams et al. (2004). However, as shown by Broadgate et al. (2000), the seasonal cycle of these compounds can vary by an order of magnitude, and should not be neglected.

Unfortunately, measurements of most tracers in the ocean are still rare. In fact, the very limited knowledge of the sea water concentration of the tracers currently represents the most important limitation in the application of this submodel.

Nevertheless, in the following we present three studies, showing the successful application of AIRSEA in a GCM. The studies have been performed with AIRSEA coupled to the atmospheric chemistry GCM ECHAM5/MESSy (Jöckel et al., 2005, Roeckner et al., 2006).

For the evaluation we first show that the simulated air-sea transfer velocity has the correct dependence on the solubility of the tracer (Sect. 4.1); then we compare simulated transfer velocities with satellite observations (Sect. 4.2); and finally we compare simulated mixing ratios of acetone with observations from a recent field campaign (Sect. 4.3).

#### 4.1 Liquid and gas phase transfer velocity

With the “resistance exchange process”, as described in Sect. 2, i.e., using the definitions Eq. (3), Eq. (4), and Eq. (11), we calculated the relative importance of gas phase and liquid phase resistance for the air-sea exchange process of CO<sub>2</sub> and CH<sub>3</sub>COCH<sub>3</sub>.

Soluble tracers have a relatively high resistance in the gas-phase, and non-soluble tracers in the liquid-phase. For CO<sub>2</sub>, for instance, the total transfer velocity depends for more than 99% on the liquid phase transfer velocity, which is the classical approximation for modelling exchange rates of this tracer. The same calculation applied to a more soluble tracer, however, shows that the gas-phase resistance plays a major role. For acetone (see Fig. 3) the gas phase transfer velocity accounts for roughly 20% of the total transfer velocity.

Title Page

Abstract

Introduction

Conclusions

References

Tables

Figures

◀

▶

◀

▶

Back

Close

Full Screen / Esc

Printer-friendly Version

Interactive Discussion

## 4.2 Transfer velocity and satellite measurements

To test the output of the model, we apply AIRSEA in ECHAM5/MESSy, whereby ECHAM5 is forced by sea-surface temperatures of AMIPII (Taylor et al., 2000) of the years 2000 to 2002. Specifying the molar volume at the boiling point of CO<sub>2</sub> (37.3 cm<sup>3</sup>/mol), and further the Henry's Law coefficient ( $A=3.6$  M/atm and  $B=2200$  K,  $H=A \times e^{[B((1/T)-(1/298.15))]}$ ) (Sander, 1999b) we obtain a simulated climatology of the transfer velocity for CO<sub>2</sub>. Figure 4 depicts the resulting annual zonal average transfer velocity  $K_{\text{tot}}$ .

The results of the simulation are similar to the climatology obtained from satellite measurements (Boutin and Etcheto, 1997; Carr et al., 2002), demonstrating the successful implementation of the algorithm. Compared to Carr et al. (2002), the overall patterns are well reproduced. The highest transfer velocity is predicted at absolute latitudes higher than 40°, while the minimum is located at the equator. The differences between the application of Eq. (7) and Eq. (8) are quite consistent. The Wanninkhof (1992) parameterization (Eq. 7) predicts higher transfer velocities with a maximum difference of 0.04 mol m<sup>-2</sup> y<sup>-1</sup> μatm<sup>-1</sup>; however, the equatorial minimum is reproduced. Moreover, a realistic seasonal cycle over the transfer velocity is simulated, further supporting the correct implementation, and showing the effect of the sea surface temperature on the exchange process. In Fig. 5 the seasonal cycle over the Pacific Ocean is depicted; the lowest exchange rates occur around the equator, and the maximum at high southern latitudes in the storm tracks where the exchange rate is very high due to the high wind speeds. A strong seasonal cycle is predicted in the subtropical region (10° N–40° N and 10° S–40° S) where the sea surface temperature amplitude is higher than in other regions.

This agreement between satellite observation and model simulation corroborates the accurate representation of the process by the submodel.

Title Page

Abstract

Introduction

Conclusions

References

Tables

Figures

◀

▶

◀

▶

Back

Close

Full Screen / Esc

Printer-friendly Version

Interactive Discussion

### 4.3 Meteor 55 ship cruise

The submodel has been further evaluated using measurements of VOCs over the tropical Atlantic Ocean during Cruise 55 of the research ship Meteor (Williams et al., 2004). During this campaign several organic compounds have been measured in air and in ocean water. The resolution used is T42L90MA (~2.8° horizontal resolution, and 90 vertical layers up to 0.1 hPa). The simulation period covers that of the campaign in autumn 2002. The set-up of the simulation is exactly the same as described in Jöckel et al. (2006) with the unique exception of the use of the AIRSEA submodel. We present a one-to-one comparison for acetone, which is moderately soluble. This means that both phases (liquid and gas) are important and influence the air-sea exchange process. This implies that acetone is one of the most complex tracers for which we can compare our model results. In the absence of a more extensive dataset, we had to make the idealised assumption of a constant concentration of acetone in sea water. This is clearly not representative for the globe, but acceptable for the region around the ship track. A constant concentration of 14 nmol/L was assumed.

Figures 6 and 7 show the distributions of point-by-point differences between model results and the observations calculated without and with AIRSEA, respectively. The improvement of the mixing ratio of acetone in air by accounting for the air-sea exchange process is obvious. With AIRSEA the difference distribution is narrower and more centered around zero. The average bias is less than 100 pmol/mol. Without AIRSEA, deviations between model and observation frequently exceed 400 pmol/mol. The root mean square deviation (RMS) confirms this visual impression. The model simulation without AIRSEA yields a RMS of 0.165 nmol/mol, while with the AIRSEA submodel the RMS is reduced to 0.061 nmol/mol.

Figure 8 shows that by applying AIRSEA, the simulated acetone mixing ratio changes strongly in the marine boundary layer. In the simulation with the new submodel the mixing ratios in the tropics are generally higher. Figure 9 shows the relative changes throughout the troposphere during a single day. In the tropics, especially south of the

Title Page

Abstract

Introduction

Conclusions

References

Tables

Figures

◀

▶

◀

▶

Back

Close

Full Screen / Esc

Printer-friendly Version

Interactive Discussion

equator where atmospheric acetone is generally lower than in the north of it, increases up to a factor of 3 are simulated. In the northern hemisphere over the Atlantic Ocean during this period the atmospheric mixing ratios generally decrease by up to 50 % or more. Although the simulated north-south distribution of acetone changes substantially the overall tropospheric mean mixing ratio changes by less than 15%.

## 5 Conclusions

The MESSy submodel AIRSEA for the calculation of the air-sea exchange of chemical constituents has been presented. The implementation of a more mechanistic approach permits an easy extension of the model to a wide variety of tracers, allowing also process studies. The realistic description of this process and the low computational requirements can be expected to improve the ability of global models to predict the chemical composition of the atmosphere. This is especially required for the interpretation of observational data, notably for data obtained on ships. Currently, the major limitation of this approach is, however, a good characterisation of the water concentration of the tracers. Additional measurements are needed to improve our knowledge in this field.

*Acknowledgements.* We are grateful to J. Williams for providing the METEOR55 data used in this paper. Thanks to the MESSy team for the good suggestions and comments. The authors wish to acknowledge the use of the Ferret program for analysis and graphics in this paper. Ferret is a product of NOAA's Pacific Marine Environmental Laboratory. (Information is available at <http://www.ferret.noaa.gov>)

## References

Asher, W. and Pankow, J.: Prediction of Gas/Water mass transport coefficients by a surface renewal model, Environ. Sci. Tech., 25, 1294–1300, 1991. 8191

Title Page

Abstract

Introduction

Conclusions

References

Tables

Figures

◀

▶

◀

▶

Back

Close

Full Screen / Esc

Printer-friendly Version

Interactive Discussion

## MESSy AIRSEA

A. Pozzer et al.

Title Page

Abstract

Introduction

Conclusions

References

Tables

Figures

◀

▶

◀

▶

Back

Close

Full Screen / Esc

Printer-friendly Version

Interactive Discussion

- Asher, W. and Wanninkhof, R.: The effect of bubble-mediated gas transfer on purposeful gaseous tracer experiments, *J. Geophys. Res.*, 103, 10555–10560, 1998a. [8193](#), [8194](#)
- Asher, W. and Wanninkhof, R.: Transient tracers and air-sea gas transfer, *J. Geophys. Res.*, 103, 15939–15958, 1998b. [8194](#)
- 5 Berner, U., Poggenburg, J., Faber, E., Quadfasel, D., and Frische, A.: Methane in ocean waters of the Bay of Bengal: its sources and exchange with the atmosphere, *Deep-Sea Res.*, 11, 925–950, doi:10.1016/S0967-0645(02)00613-6, 2003. [8190](#)
- Boutin, J. and Etcheto, J.: Long-term variability of the air-sea CO<sub>2</sub> exchange coefficient: Consequence for the CO<sub>2</sub> fluxes in the equatorial Pacific Ocean, *Global Biogeochem. Cycles*, 11, 453–470, 1997. [8200](#)
- 10 Boyer, T., Stephens, C., Antonov, J., Conkright, M., Locarnini, R., O'Brien, T., and Garcia, H.: *World Ocean Atlas 2001, Volume 2: Salinity*, 167 pp., NOAA Atlas NESDIS 50, U.S. Government Printing Office, 2002. [8193](#)
- Broadgate, W., Liss, P., and Penkett, A.: Seasonal emission of isoprene and other reactive hydrocarbon gases from the ocean, *Geophys. Res. Lett.*, 24, 2675–2678, 2000. [8199](#)
- 15 Carpenter, L., Alastair, C., and Hopkin, J.: Uptake of methanol to the North Atlantic Ocean surface, *Global Biogeochem. Cycles*, 18, GB4027, doi:10.1029/2004GB002294, 2004. [8190](#), [8195](#)
- Carr, M.-E., Wenqing, T., and Liu, W.: CO<sub>2</sub> exchange coefficients from remotely sensed wind speed measurements: SSM/I versus QuikSCAT in 2000, *Geophys. Res. Lett.*, 29, 15, doi:10.1029/2002GL015068, 2002. [8200](#)
- 20 Garland, J.: The dry deposition of sulphur dioxide to land and water surfaces, *Proc. R. Soc. London*, 354, 245–268, 1977. [8195](#)
- Hayduk, W. and Laudie, H.: Prediction of diffusion coefficients for nonelectrolytes in dilute aqueous solutions, *AIChE J.*, 20, 611–615, 1974. [8195](#)
- Ho, D., Zappa, C., McGills, W., Bliven, L., Ward, B., Dacey, J., Schlosser, P., and Hendricks, M.: influence of rain on air-sea gas exchange: Lesson from a model ocean, *J. Geophys. Res.*, 109, C08S18, doi:10.1029/2003JC001806, 2004. [8194](#)
- 25 Jähne, B., Muennich, K., Boesinger, R., Dutzi, A., Huber, W., and Libner, P.: On parameter influencing the air-water gas exchange, *J. Geophys. Res.*, 92, 1937–1949, 1987. [8193](#)
- Jöckel, P., Sander, R., Kerkweg, A., Tost, H., and Lelieveld, J.: Technical Note: The Modular Earth Submodel System (MESSy) – a new approach towards Earth System Modeling, *Atmos. Chem. Phys.*, 5, 433–444, 2005. [8190](#), [8197](#), [8199](#)

Jöckel, P., Sander, R., Kerkweg, A., Tost, H., and Lelieveld, J.: Evaluation of the atmospheric chemistry GCM ECHAM5/MESSy: Consistent simulation of ozone in the stratosphere and troposphere, *Atmos. Chem. Phys. Discuss.*, 6, 6957–7050, 2006.

5 Kerkweg, A., Sander, R., Tost, H., and Jöckel, P.: Technical Note: Implementation of prescribed (OFFLEM), calculated (ONLEM), and pseudo-emissions (TNUDGE) of chemical species in the Modular Earth Submodel System (MESSy), *Atmos. Chem. Phys. Discuss.*, 6, 5485–5504, 2006.

Kettle, A. J. and Andreae, M.: Flux of dimethylsulfide from the oceans: A comparison of updated data set and flux models, *J. Geophys. Res.*, 105, 26 793–26 808, 2000. [8190](#)

10 Liss, P. and Merlivat, L.: Air-sea gas exchange rates: Introduction and synthesis, in *The Role of Air-Sea Exchange in Geochemical Cycling*, 113–127, P. Buat-Menard, 1986. [8193](#)

Liss, P. and Slater, P.: Flux of gases across the air-sea interface, *Nature*, 247, 181–184, 1974. [8191](#), [8192](#)

15 Lyman, W., Reehl, W., and Rosenblatt, D.: *Handbook of chemical property estimation methods*, American Chemical Society, Washington DC, USA, 1990. [8196](#)

Marandino, C., De Bruyn, W., Miller, S., Prather, M., and Saltzmann, E.: Oceanic uptake and the global atmospheric acetone budget, *Geophys. Res. Lett.*, 32, L15806, doi:10.1029/2005GL023285, 2005. [8190](#)

20 Monahan, E.: Occurrence and evolution of acoustically relevant sub surface bubble plumes and their associated, remotely monitorable, surface withcaps, in *Natural Physical Sources of Underwater Sound*, edited by: Kerman, B., 503–517, Kluwer Acad., 1993. [8193](#)

Nightingale, P. D., Malin, G., Law, C. S., Watson, A. J., Liss, P. S., Liddicoat, M. I., Boutin, J., and Upstill-Goddard, R. C.: In situ evaluation of air-sea gas exchange parametrizations using novel conservative and volatile tracers, *Global Biogeochem. Cycles*, 14, 373–387, 2000. [8193](#)

25 Plass-Dülmer, C., Koppman, R., Ratte, M., and Rudolph, J.: Light nonmethane hydrocarbons in seawater, *Global Biogeochem. Cycles*, 9, 79–100, 1995. [8190](#), [8199](#)

Roeckner, E., Brokopf, R., Esch, M., Giorgetta, M., Hagemann, S., Kornblueh, L., Manzini, E., Schlese, U., and Schulzweida, U.: Sensitivity of simulated climate to horizontal and vertical resolution in the ECHAM5 atmosphere model, *J. Clim.*, 3771–3791, 2006. [8199](#)

30 Saltzmann, E., King, D., Holman, K., and Leck, C.: Experimental determination of the diffusion coefficient of dimethylsulfide in water, *J. Geophys. Res.*, 98, 16 481–16 486, 1993. [8195](#)

Sander, R.: Modeling atmospheric chemistry: Interactions between gas-phase species and

---

MESSy AIRSEA

A. Pozzer et al.

---

Title Page

Abstract

Introduction

Conclusions

References

Tables

Figures

◀

▶

◀

▶

Back

Close

Full Screen / Esc

Printer-friendly Version

Interactive Discussion

## MESSy AIRSEA

A. Pozzer et al.

Title Page

Abstract

Introduction

Conclusions

References

Tables

Figures

◀

▶

◀

▶

Back

Close

Full Screen / Esc

Printer-friendly Version

Interactive Discussion

liquid cloud/aerosol particles, *Surv. Geophys.*, 20, 1–31, 1999a. [8191](#)

Sander, R.: Compilation of Henry's law constant for inorganic and organic species of potential importance in environmental chemistry, <http://www.henrys-law.org>, 1999b. [8191](#), [8200](#)

Singh, H., Chen, Y., Staudt, A. C., Jacob, D. J., Blake, D. R., Heikes, B. G., and Snow, J.: Evidence from the Pacific troposphere for large global sources of oxygenated organic compounds, *Nature*, 410, 1078–1081, 2001. [8190](#)

Soloviev, A. and Schluessel, P.: A model of air-sea gas exchange incorporating physics of the turbulent boundary layer and the properties of the sea surface, in *Gas transfer at water surface*, edited by M. Donelan, W. Drennan, M. Saltzmann, and R. Wanninkhof, 141–146, *Geophys. Monogr.*, 2002. [8193](#)

Taylor, K., Williamson, D., and Zwiers, F.: The sea surface temperature and sea ice concentration boundary conditions for AMIP II simulations; PCMDI Report, Tech. Rep. 60, Program for Climate Model Diagnosis and Intercomparison, 2000. [8200](#)

Wanninkhof, R.: Relationship between wind speed and gas exchange over the ocean, *J. Geophys. Res.*, 97, 7373–7382, 1992. [8193](#), [8196](#), [8200](#)

Wesely, M.: Parametrization of surface resistances to gaseous dry deposition in regional-scale numerical models, *Atmos. Environ.*, 23, 1293–1304, 1989. [8195](#)

Wilke, C. and Chang, P.: Correlation of diffusion coefficients in dilute solutions, *AIChE J.*, 1, 264–270, 1955. [8195](#)

Williams, J., Holzinger, R., Gros, V., Xu, X., Atlas, E., and Wallace, D.: Measurements of organic species in air and seawater from the tropical Atlantic, *Geophys. Res. Lett.*, 31, L23S06, doi:10.1029/2004GL02001, 2004. [8199](#), [8201](#)

Xie, W., Su, J., and Xie, X.: Studies on the activity coefficients of benzene and its derivatives in aqueous salt solution., *Thermochimica Acta*, 169, 271–286, 1990. [8192](#)

Xie, W., Shiu, W., and Mackay, D.: A review of the effect of salt on the solubility of organic compounds in seawater, *Mar. Environ. Res.*, 44, 429–444, 1997. [8192](#), [8193](#)

Zhou, X. and Mopper, K.: Carbonyl compounds in the lower marine troposphere over the Caribbean sea and Bahamas, *J. Geophys. Res.*, 98, 2385–2392, 1993. [8199](#)

Zhou, X. and Mopper, K.: Photochemical production of low-molecular weight compounds in seawater and surface microlayer and their air-sea exchange, *Mar. Chem.*, 56, 201–213, 1997. [8199](#)

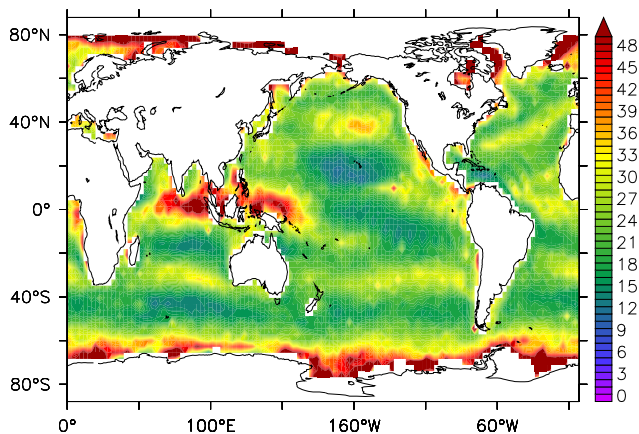


**Fig. 1.** Annual average time scale  $\tau$  of air-sea exchange for  $\text{CO}_2$  in days. The height of the lowest model layer is  $\approx 60$  m.

[Title Page](#)[Abstract](#)[Introduction](#)[Conclusions](#)[References](#)[Tables](#)[Figures](#)[◀](#)[▶](#)[◀](#)[▶](#)[Back](#)[Close](#)[Full Screen / Esc](#)[Printer-friendly Version](#)[Interactive Discussion](#)

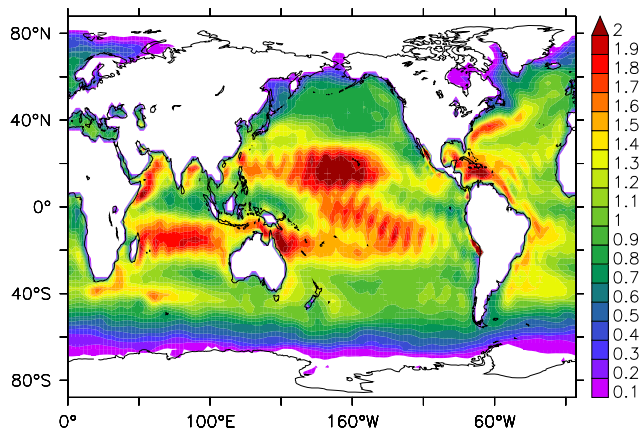


**Fig. 2.** Annual average transfer velocity  $K_{tot}$  for  $\text{CH}_3\text{OH}$  in  $\mu\text{m/s}$ .

[Title Page](#)[Abstract](#)[Introduction](#)[Conclusions](#)[References](#)[Tables](#)[Figures](#)[◀](#)[▶](#)[◀](#)[▶](#)[Back](#)[Close](#)[Full Screen / Esc](#)[Printer-friendly Version](#)[Interactive Discussion](#)

EGU

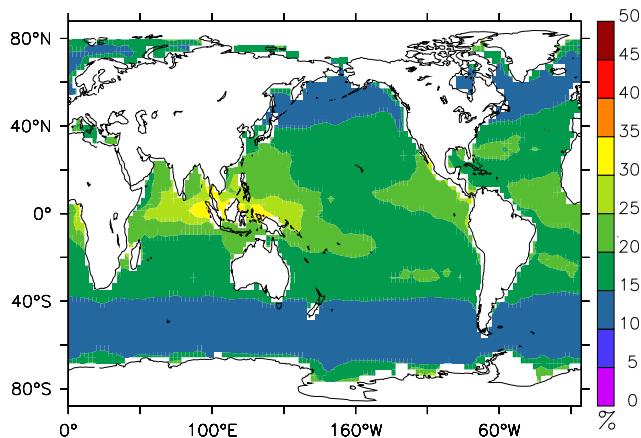


**Fig. 3.** Simulated annual average ratio between water and total resistance ( $K_{tot}/K_w$ ) for acetone ( $CH_3COCH_3$ ).

[Title Page](#)[Abstract](#)[Introduction](#)[Conclusions](#)[References](#)[Tables](#)[Figures](#)[◀](#)[▶](#)[◀](#)[▶](#)[Back](#)[Close](#)[Full Screen / Esc](#)[Printer-friendly Version](#)[Interactive Discussion](#)

EGU

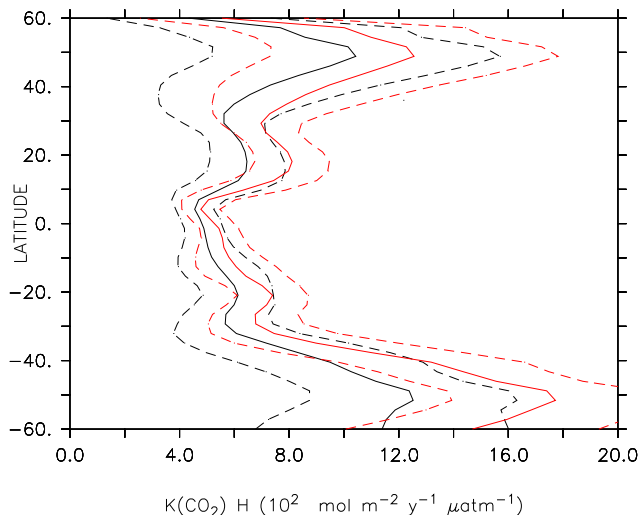


**Fig. 4.** Simulated annual zonal average transfer velocity for  $\text{CO}_2$ . The red line shows the results obtained with Eq. (7), the black line shows the results for which the whitecap parameterization (Eq. 8) has been selected. Dashed lines are the standard deviations indicating the simulated variability in one year. The results are not weighted by ocean surface.

[Title Page](#)[Abstract](#)[Introduction](#)[Conclusions](#)[References](#)[Tables](#)[Figures](#)[◀](#)[▶](#)[◀](#)[▶](#)[Back](#)[Close](#)[Full Screen / Esc](#)[Printer-friendly Version](#)[Interactive Discussion](#)

EGU

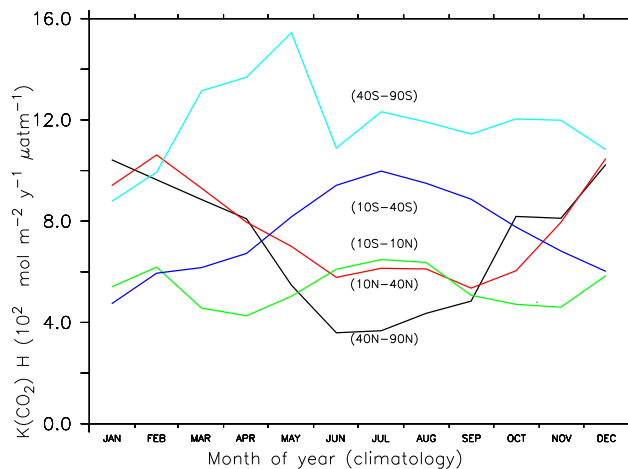


**Fig. 5.** Simulated seasonal cycle of the transfer velocity of CO<sub>2</sub> over the Pacific Ocean for different latitude bands.

[Title Page](#)[Abstract](#)[Introduction](#)[Conclusions](#)[References](#)[Tables](#)[Figures](#)[◀](#)[▶](#)[◀](#)[▶](#)[Back](#)[Close](#)[Full Screen / Esc](#)[Printer-friendly Version](#)[Interactive Discussion](#)

EGU

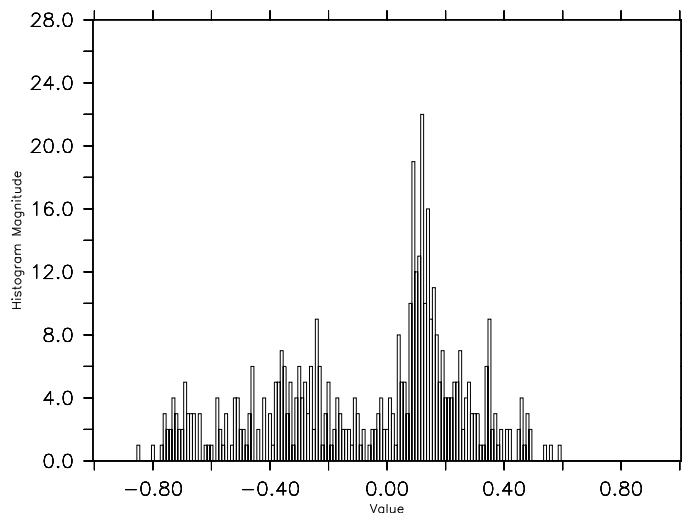


**Fig. 6.** Histogram of differences between the observations and the ECHAM5/MESSy simulation (T42L90MA, reference simulation) without the submodel AIRSEA. in nmol/mol.

[Title Page](#)[Abstract](#)[Introduction](#)[Conclusions](#)[References](#)[Tables](#)[Figures](#)[◀](#)[▶](#)[◀](#)[▶](#)[Back](#)[Close](#)[Full Screen / Esc](#)[Printer-friendly Version](#)[Interactive Discussion](#)

EGU

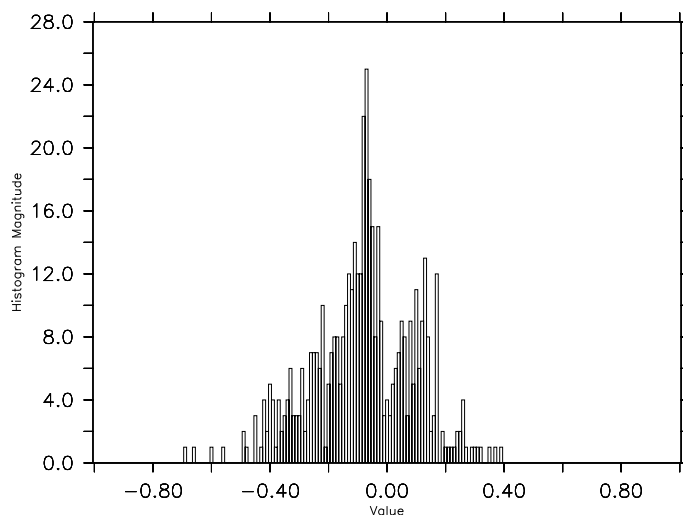


**Fig. 7.** Histogram of differences between the observations and the ECHAM5/MESSy simulation (T42L90MA) with the submodel AIRSEA in nmol/mol.

[Title Page](#)[Abstract](#)[Introduction](#)[Conclusions](#)[References](#)[Tables](#)[Figures](#)[◀](#)[▶](#)[◀](#)[▶](#)[Back](#)[Close](#)[Full Screen / Esc](#)[Printer-friendly Version](#)[Interactive Discussion](#)

EGU

## MESSy AIRSEA

A. Pozzer et al.

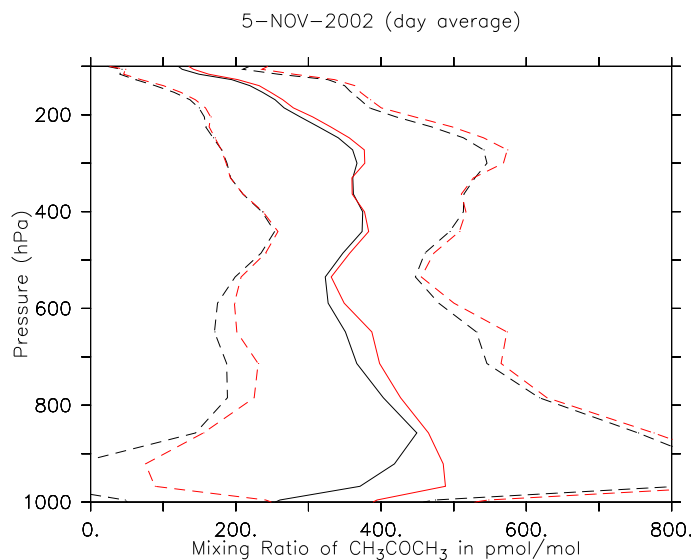


**Fig. 8.** Example of the vertical profile simulated by ECHAM5/MESSy (T42L90MA, reference simulation, in black) and ECHAM5/MESSy with the submodel AIRSEA (red)  $\text{CH}_3\text{COCH}_3$ . The profiles represent one day average over the region where the campaign METEOR55 took place. The dashed lines represent the spatial standard deviation.

[Title Page](#)[Abstract](#)[Introduction](#)[Conclusions](#)[References](#)[Tables](#)[Figures](#)[◀](#)[▶](#)[◀](#)[▶](#)[Back](#)[Close](#)[Full Screen / Esc](#)[Printer-friendly Version](#)[Interactive Discussion](#)

EGU

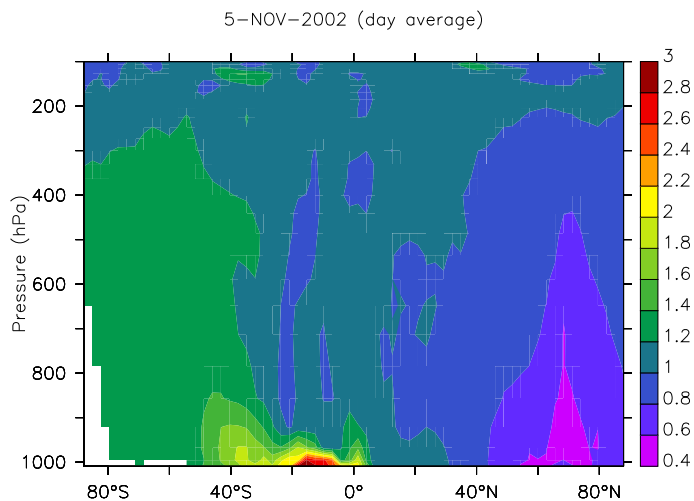


**Fig. 9.** Relative change in the acetone mixing ratio comparing the submodel AIRSEA in ECHAM5/MESSy with the reference simulation for one day in November 2002. The values have been zonally averaged over the Atlantic Ocean.

[Title Page](#)[Abstract](#)[Introduction](#)[Conclusions](#)[References](#)[Tables](#)[Figures](#)[◀](#)[▶](#)[◀](#)[▶](#)[Back](#)[Close](#)[Full Screen / Esc](#)[Printer-friendly Version](#)[Interactive Discussion](#)

EGU